

# Structural, Morphological And Room Temperature Dielectric Properties Of $\text{CoNd}_x\text{Fe}_{2-x}\text{O}_4$ Nanomaterials Obtained Via Citrate-Gel Auto-Combustion Method

Sathish Boddolla\*<sup>1</sup>, D Ravinder<sup>1</sup>

<sup>1</sup> Dept Of Physics, Osmania University, Hyderabad, 500007.

---

## Abstract:

Here we reporting the structural and magnetic properties of neodymium-doped cobalt ferrites with general formula  $\text{CoNd}_x\text{Fe}_{2-x}\text{O}_4$  (where  $x=0, 0.02, 0.04, 0.06, 0.08, \text{ and } 0.10$ ) nanomaterials obtained from sol-gel auto-combustion method. The obtained precursors were calcined at 773 K/4 h. The crystal structure of calcined powders was analyzed using X-ray diffraction (XRD), and morphological studies were done by scanning electron microscopy (SEM). The peaks obtained from the XRD confirmed the single-phase spinel ferrite structure without any secondary impurity phases. The lattice parameter, cell volume, density, and crystallite size were calculated for all the samples using XRD data. Crystallite size was decreased from 19 nm to 12.8 nm with an increase of Nd concentration (from 0 to 0.10). SEM studies show that the particles are irregularly shaped grains morphology with a homogeneous distribution.

**Keywords:** Cobalt ferrite, Neodymium, XRD, SEM, Dielectric loss, Activation energy .

---

Date of Submission: 11-04-2024

Date of Acceptance: 21-04-2024

---

## I. Introduction:

The spinel ferrite nanoparticle with a general formula of  $\text{MFe}_2\text{O}_4$  (where  $\text{M} = \text{Fe, Co, Cu, Mn, etc.}$ ) has drawn much attention from the research point of view due to their unique physical, chemical, and magnetic properties [1-4]. Among them, the cobalt ferrite ( $\text{CoFe}_2\text{O}_4$ ) is well recognized magnetic material because of its chemically stable, mechanical hardness, high saturation magnetization, high resistivity, high coercive field, and low dielectric loss behaviors [5-7]. As a consequence, this material is considered for many applications, such as high-density magnetic recording, magnetic fluids, electronic devices, gas sensors, catalysis, medicine, microwave devices, etc., [8-15]. The properties of this material can be further tuned by adding a dopant into their structure, sintering temperature, synthesis method, and changing their particle size [16-18]. Nanocrystalline of doped ferrites especially rare earth metals have interesting technical and physical applications [19]. Doping of rare earth ions into cobalt ferrite leads to structural distortion that induces strains in the material which indicates improved crystallinity of the sample and to effect the structural, electrical, and magnetic properties significantly [20].

## II. Sample preparation

Cobalt (II) nitrate hexahydrate, iron (III) nitrate nonahydrate, neodymium (III) nitrate hexahydrate, and citric acid were used as starting materials. The flow chart for the synthesis of  $\text{CoNd}_x\text{Fe}_{2-x}\text{O}_4$  ( $0 \leq x \leq 0.1$ ). To begin with, suitable amounts of cobalt nitrate, iron nitrate, and neodymium nitrate were mixed in deionized water under continuous stirring. The citric acid in a 3:1 molar ratio for precursors was added to the solution as a chelating agent and stirred for 2 hours to get a homogeneous mixture of metal nitrates. The pH~7 of the above solution was maintained by adding the ammonia solution drop by drop with continuous stirring. The resultant solution was continuously heated on the hot plate at 100°C up to dryness with continuous stirring, as a result, a viscous gel was obtained. Further, the temperature was increased up to 200°C, and this temperature led to the ignition of the gel. The dried gel burnt completely in a self-propagating combustion manner to form a loose powder. Then the powder was ground and calcined at 500°C for 4 h to achieve the final product.

## III. Characterization

$\text{Nd}^{3+}$  doped Cobalt samples were characterized by the X-ray diffraction (XRD) technique for structure identification and phase purity using the model (X-ray Diffraction System Ultima IV of Rigaku Corporation, Japan). XRD patterns were recorded using  $\text{Cu-K}\alpha$  radiation ( $\lambda=1.540598\text{\AA}$ ) operated at 45kV with 40mA in the  $2\theta$  range 20 to 800. The microstructural morphology and grain distribution were investigated by a scanning electron microscope (SEM) Hitachi S3400N operated at 15kV. In order have extended

electrical contacts, the copper leads were bonded firmly on both sides of silver electroded pellets and dried at 150 oC/ 12h. The capacitance (Cp) and loss (D) of each pellet were recorded for a wide range of frequencies (100 Hz to 10 MHz) at room temperature using a Impedance analyzer (WAYNE KERR, 6500B), attached to a home built furnace connected to a programmable temperature controller.

#### IV.Result And Discussion

##### XRD analysis of $\text{Nd}^{3+}$ doped $\text{CoFe}_2\text{O}_4$ :

Fig.1 shows the room temperature XRD patterns of  $\text{CoNd}_x\text{Fe}_{2-x}\text{O}_4$  ( $x=0, 0.02, 0.04, 0.06, 0.08$  and  $0.10$ ) nanomaterials. These results were compared with standard JCPDS (card No. 22-1086). The XRD pattern confirms the formation of a single-phase FCC spinal structure up to the Nd concentration  $x=0.02$ . The intensity of the XRD peak decreases with further addition of  $\text{Nd}^{3+}$  concentration, and this infers that crystallization is a difficulty due to relatively large ion radii[21 22]

Scherrer-Debye equation was used to calculate the average crystallite size (D) of all samples

$$D = \frac{0.91 \cdot \lambda}{\beta \cos \theta} \quad (1)$$

The lattice constant a is calculated using Braggs equation (2) from the high-intensity peak (311).

$$a = d \sqrt{h^2 + k^2 + l^2} \quad (2)$$

The actual X-ray density was also determined using equation

$$\rho_x = \frac{8M}{Na^3} \quad (3)$$

where (M) is the molecular weight, (N) is Avogadro's number, and (a) is the lattice parameter. The calculated average crystallite size, lattice constant, and X-ray density of all the samples were mentioned in Tab.1. This table indicates that the lattice parameters and crystallite sizes were decreased and x-ray density was increased with an increase of  $\text{Nd}^{3+}$  concentration. This is due incorporation of large ionic radii.

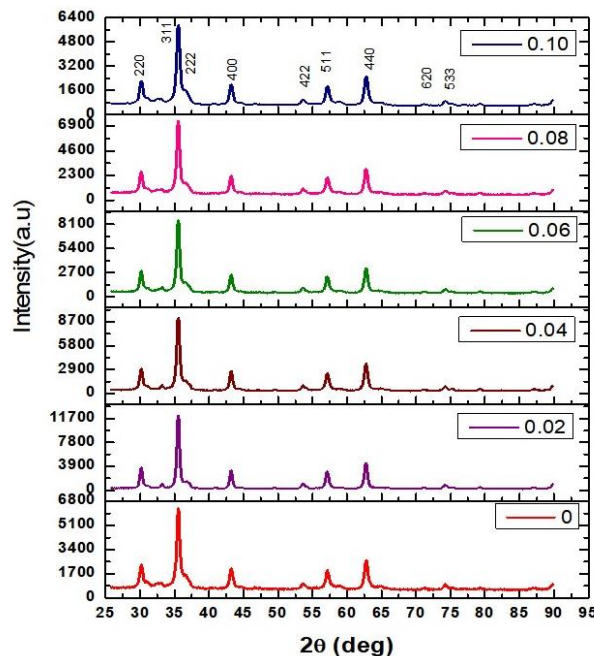


Fig.1 XRD patterns of  $\text{Nd}^{3+}$  doped  $\text{CoFe}_2\text{O}_4$ .

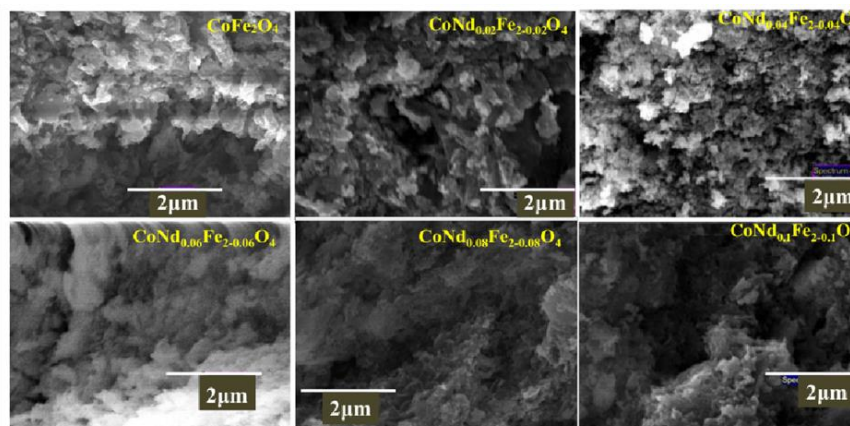
Tab.1: Calculated lattice constant, crystallite size, X-ray density and volume of  $\text{CoNd}_x\text{Fe}_{2-x}\text{O}_4$  nanomaterials using XRD data.

S No	Composition x	Lattice Constant "a" (Å)	Crystallite size (D) nm	X-ray Density ( $\rho_x$ )	Volume (V)
1	0	8.37142	19.086	5.312	586.675
2	0.02	8.37164	16.024	5.352	586.721

3	0.04	8.37007	13.957	5.394	586.392
4	0.06	8.37008	14.028	5.435	586.393
5	0.08	8.37000	13.654	5.475	586.377
6	0.10	8.36736	12.806	5.520	585.823

**SEM studies of Nd<sup>3+</sup> doped Cobalt ferrites:**

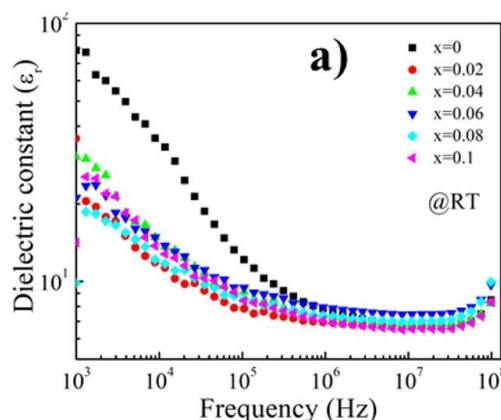
The surface morphology of  $\text{CoNd}_x\text{Fe}_{2-x}\text{O}_4$  ( $0 < x < 0.1$ ) were shown in Fig.2. These surface morphologies reflect the homogeneous distribution of multi-shaped grains without segregation at the grain boundaries. The average grain size was closely 20 nm and slightly fluctuate the size with the substitution of Nd concentration[23].



**Dielectric Studies of Nd<sup>3+</sup> doped Cobalt ferrites:**

The physical properties especially dielectric properties of  $\text{CoFe}_2\text{O}_4$  based materials are mainly depend on the purity, crystallite size, dopant concentration, content of  $\text{Fe}^{3+}/\text{Fe}^{2+}$  ions, microstructure and the processing conditions during the preparation.

To investigate the dielectric properties of  $\text{Nd}^{3+}$  doped  $\text{CoFe}_2\text{O}_4$  samples, the impedance studies of the each material under this study were carried out at different temperatures. The typical plots at room temperature of the dielectric constant ( $\epsilon_r$ ), the loss ( $\tan\delta$ ), and conductivity as a function of frequency for the  $\text{Nd}^{3+}$  doped  $\text{CoFe}_2\text{O}_4$  samples were depicted in Fig.3(a-c). Fig.3(a) shows that the dielectric constant is decreasing from 103-106 and further the value is almost the same, which is the ordinary behavior of ferrite compounds. Furthermore the dielectric constant was decreased with increase of  $\text{Nd}^{3+}$  concentrations, and this may be attributed to the decrease of  $\text{Fe}^{3+}$  ion content in the samples[24]. Due to the reduced space charge polarization caused by the dopants ability to prevent electrons moving between the  $\text{Fe}^{2+}$  and  $\text{Fe}^{3+}$  ions in the samples. The dielectric loss of all the samples was also investigated and these values are decreasing with an increase in frequency (Fig.3(b)). However, the conductivity is increasing with the increase in frequency (Fig.3(c)) of the all the samples. Furthermore the conductivity was decreased with increase of  $\text{Nd}^{3+}$  concentrations, which is due to the decrease of  $\text{Fe}^{2+}$  ion content in the  $\text{CoFe}_2\text{O}_4$  samples[25 26].



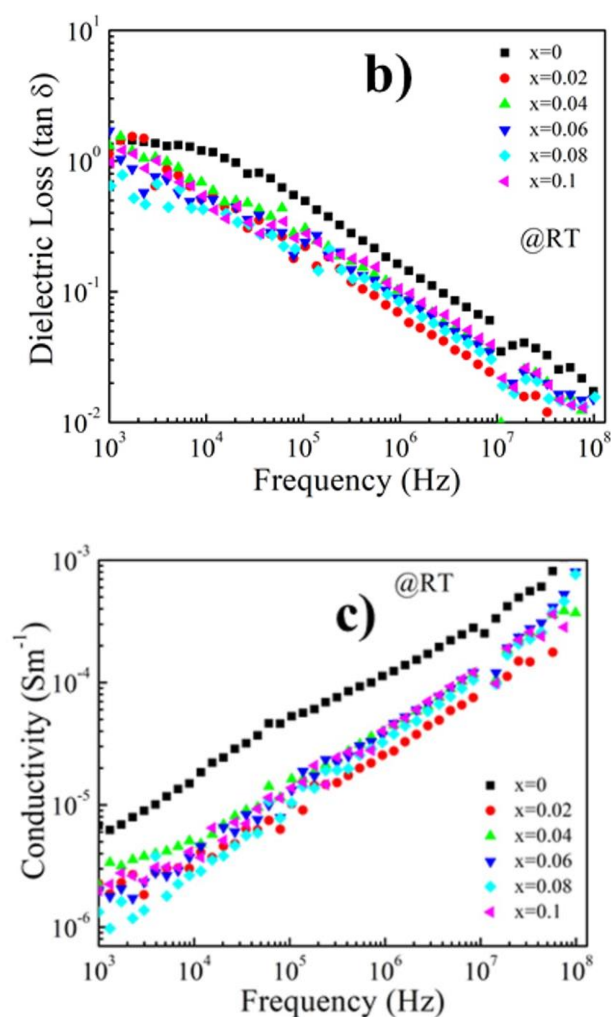


**Fig.3 Room temperature a) Dielectric constant, b) dielectric loss and c) conductivity of the  $\text{CoNd}_x\text{Fe}_{2-x}\text{O}_4$  nanomaterials**

### V. Conclusions:

In this work, we demonstrated structural, morphological and dielectric properties of the  $\text{Nd}^{3+}$ -doped cobalt ferrite nanoparticles derived from a citrate-assisted sol-gel auto-combustion method. XRD reveals that the pure spinel crystalline structure was formed up to 0.02 mol of  $\text{Nd}^{3+}$  doping, and with further increase of  $\text{Nd}^{3+}$  concentrations, the crystallinity was difficult. High grain boundary activation energy was observed for the  $\text{CoFe}_{1.98}\text{Nd}_{0.02}\text{O}_4$  nanomaterials. The obtained results of  $\text{CoFe}_{1.98}\text{Nd}_{0.02}\text{O}_4$  nanomaterials will be a good candidate for different applications.

### References

- [1] L. Zhao, X. Li, Q. Zhao, Z. Qu, D. Yuan, S. Liu, X. Hu, Guohuachensynthesis, Characterization And Adsorptive Performance Of  $\text{MgFe}_2\text{O}_4$  Nanospheres For  $\text{SO}_2$  Removal, *J. Hazardous Materials* (2010), 184, 704-709. <https://doi.org/10.1016/j.jhazmat.2010.08.096>
- [2] M.J. Uddin, Y.-K. Jeong, Application Of Magnesium Ferrite Nanomaterials For Adsorptive Removal Of Arsenic From Water: Effects Of Mg And Fe Ratio, *Chemosphere* (2022), 307, 135817. <https://doi.org/10.1016/j.chemosphere.2022.135817>
- [3] K.-X. Shi, F. Qiu, P. Wang, H. Li, C.-C. Wang, Magnetic  $\text{MgFe}_2\text{O}_4/\text{MIL-88A}$  Catalyst For Photo-Fenton Sulfamethoxazole Decomposition Under Visible Light, *Separation And Purification Technology*, (2022), 301, 121965. <https://doi.org/10.1016/j.seppur.2022.121965>
- [4] S. Zhang, H. Niu, Y. Cai, X. Zhao, Y. Shi, Arsenite And Arsenate Adsorption On Coprecipitated Bimetal Oxide Magnetic Nanomaterials:  $\text{MnFe}_2\text{O}_4$  And  $\text{CoFe}_2\text{O}_4$ , *Chemical Engineering Journal* (2010) 158, 99-607. <https://doi.org/10.1016/j.cej.2010.02.013>
- [5] T.L. Templeton, A.S. Arrott, A.E. Curzon, M.A. Gee, X. - Z. Li, Y. Yoshida, P.J. Schurer, J.L. Lacombe, Magnetic Properties Of  $\text{CoFe}_3\text{-Xo}_4$  During Conversion From Normal To Inverse Spinel Particles, *J. Applied Physics* (1993) 73, 6728. <https://doi.org/10.1063/1.352516>
- [6] P. Sivagurunathan, S.R. Gibin, Preparation And Characterization Of Nanosized Cobalt Ferrite Particles By Co-Precipitation Method With Citrate As Chelating Agent, *J Mater Sci: Mater Electron* (2016) 27, 8891-8898. <https://doi.org/10.1007/S10854->

- 016-4915-5
- [7] S. Ayyappan, S. Mahadevan, P. Chandramohan, M. P. Srinivasan, J. Philip, B. Raj, Influence Of Co<sup>2+</sup> Ion Concentration On The Size, Magnetic Properties, And Purity Of CoFe<sub>2</sub>O<sub>4</sub> Spinel Ferrite Nanoparticles, *J. Phys. Chem. C* (2010) 114, 6334–6341. <https://doi.org/10.1021/Jp911966p>
- [8] H.Y. Hafeez, S.K. Lakhera, N. Narayanan, S. Harish, Y. Hayakawa, B.-K. Lee, B. Neppolian, Environmentally Sustainable Synthesis Of A CoFe<sub>2</sub>O<sub>4</sub>-TiO<sub>2</sub>/RGO Ternary Photocatalyst: A Highly Efficient And Stable Photocatalyst For High Production Of Hydrogen (Solar Fuel). *ACS Omega* (2019) 4, 880-891. <https://doi.org/10.1021/acsomega.8b03221>
- [9] M. Kooti, M. Afshari, Magnetic Cobalt Ferrite Nanoparticles As An Efficient Catalyst For Oxidation Of Alkenes, *Scientia Iranica*, (2012), 19, 1991-1995. <https://doi.org/10.1016/j.scient.2012.05.005>
- [10] T. Sathitwitayakul, K. Maxim, P. Ivan, R.B. Parkin, The Gas Sensing Properties Of Some Complex Metal Oxides Prepared By Self-Propagating High-Temperature Synthesis. *Mater. Lett.* (2012) 75, 36–38. <https://doi.org/10.1016/j.matlet.2012.02.003>
- [11] N. Momen, M. Pileni, Control Of The Size Of Cobalt Ferrite Magnetic Fluid. *J. Phys. Chem.* (1996) 100, 1867–1873. <https://doi.org/10.1021/Jp9524136>
- [12] Y. Cedeno-Mattei, O. Perales-Perez, M. Tomar, F. Roman, P. Voyles, W. Stratton, Tuning Of Magnetic Properties In Cobalt Ferrite Nanocrystals. *J. Appl. Phys.* (2008) 103, 512–513. <https://doi.org/10.1063/1.2838215>
- [13] V.S. Kumbhar, A.D. Jagdale, N.M. Shinde, C.D. Lokhande, Chemical Synthesis Of Spinel Cobalt Ferrite (CoFe<sub>2</sub>O<sub>4</sub>) Nano-Flakes For Supercapacitor Application. *Appl. Surf. Sci.* (2012) 259, 39–43. <https://doi.org/10.1016/j.apsusc.2012.06.034>
- [14] L. Lv, X. Qun, R. Ding, L. Qi, H. Wang, Chemical Synthesis Of Mesoporous CoFe<sub>2</sub>O<sub>4</sub> Nanoparticles As Promising Bifunctional Electrode Materials For Supercapacitors. *Mater. Lett.* (2013) 111, 35–38. <https://doi.org/10.1016/j.matlet.2013.08.055>
- [15] K. Yang, W. Wang, F. Dong, D. Licheng, Y. Deng, P. He, Reduced Graphene Oxide CoFe<sub>2</sub>O<sub>4</sub> Composites For Supercapacitor Electrode. *Russ. J. Electrochem.* (2013) 49, 359–364. <https://doi.org/10.1134/S1023193512080150>
- [16] R. Zhang, L. Suna, Z. Wang, W. Hao, E. Cao, Y. Zhang, Dielectric And Magnetic Properties Of CoFe<sub>2</sub>O<sub>4</sub> Prepared By Sol-Gel Auto-Combustion Method, *Materials Research Bulletin* (2018) 98, 133-138. <https://doi.org/10.1016/j.materresbull.2017.08.006>
- [17] S.I. Ahmad, Nano Cobalt Ferrites: Doping, Structural, Low-Temperature, And Room Temperature Magnetic And Dielectric Properties – A Comprehensive Review, *J. Magnetism And Magnetic Materials* (2022), 562, 169840 . <https://doi.org/10.1016/j.jmmm.2022.169840>
- [18] C. Murugesan, L. Okras, K. Ugendar, G. Chandrasekaran, X. Liu, D. Diao, J. Shen, Improved Magnetic And Electrical Properties Of Zn Substituted Nanocrystalline MgFe<sub>2</sub>O<sub>4</sub> Ferrite, *J. Magnetism And Magnetic Materials* (2022) 550, 169066. <https://doi.org/10.1016/j.jmmm.2022.169066>
- [19] R.C. Kambale, K.M. Song, Y.S. Koo, N. Hur, Low Temperature Synthesis Of Nanocrystalline Dy<sup>3+</sup> Doped Cobalt Ferrite: Structural And Magnetic Properties, *J. Applied Physics* (2011) 110, 053910. <https://doi.org/10.1063/1.3632987>
- [20] G. Bulai, L. Diamandescu, I. Dumitru, S. Gurlui, M. Feder, O.F. Caltun, Effect Of Rare Earth Substitution In Cobalt Ferrite Bulk Materials, *J. Magnetism And Magnetic Materials* (2015) 390, 123-131. <https://doi.org/10.1016/j.jmmm.2015.04.089>
- [21] A. Ghasemi, M. Mousavinia, Structural And Magnetic Evaluation Of Substituted Ni<sub>2</sub>Fe<sub>2</sub>O<sub>4</sub> Particles Synthesized By Conventional Sol–Gel Method, *Ceramics International* (2014) 40, 2825- 2834. <https://doi.org/10.1016/j.ceramint.2013.10.031>
- [22] S. Jabez, S. Mahalakshmi, S. Nithyanantham, Frequency And Temperature Effects On Dielectric Properties Of Cobalt Ferrite, *J Mater Sci: Mater Electron* (2017) 28, 5504–5511. <https://doi.org/10.1007/S10854-016-6212-8>
- [23] P.P. Goswami, H.A. Choudhury, S. Chakma, V.S. Moholkar, Sonochemical Synthesis Of Cobalt Ferrite Nanoparticles. *Int. J. Chem. Eng.* (2013). [doi:10.1155/2013/934234](https://doi.org/10.1155/2013/934234)
- [24] R. Jabbar, S.H. Sabeeh, A.M. Hameed, Structural, Dielectric And Magnetic Properties Of Mn<sup>2+</sup> Doped Cobalt Ferrite Nanoparticles, *J. Magnetism And Magnetic Materials* (2020) 494, 165726. <https://doi.org/10.1016/j.jmmm.2019.165726>
- [25] L.B. Tahar, M. Artus, S. Ammar, L.S. Smiri, F. Herbst, M.-J. Vaulay, V. Richard, J.-M. Grenèche, F. Villain, F. Fiévet, Magnetic Properties Of CoFe<sub>1.9</sub>Re<sub>0.1</sub>O<sub>4</sub> Nanoparticles (Re=La, Ce, Nd, Sm, Eu, Gd, Tb, Ho) Prepared In Polyol, *J. Magnetism And Magnetic Materials* (2008) 320, 3242-3250. <https://doi.org/10.1016/j.jmmm.2008.06.031>
- [26] R.C. Kambale, P.A. Shaikh, S. Kamble, Y.D. Kolekar, Effect Of Cobalt Substitution On Structural, Magnetic And Electric Properties Of Nickel Ferrite, *J. Alloy. Comp.* (2009) 478, 599- 603. <https://doi.org/10.1016/j.jallcom.2008.11.101>